Organic & Biomolecular Chemistry

Accepted Manuscript

This article can be cited before page numbers have been issued, to do this please use: M. Giletto, P. Osmulski, C. Jones, M. Gaczynska and J. J. Tepe, *Org. Biomol. Chem.*, 2019, DOI: 10.1039/C9OB00122K.

ROYAL SOCIETY OF CHEMISTRY

rsc.li/obc

View Article Online
DOI: 10.1039/C9OB00122K

Organic and Bioorganic Chemistry

ARTICLE

Pipecolic Esters as Minimized Templates for Proteasome Inhibition

Received 00th January 20xx,
Accepted 00th January 20xx

DOI: 10.1039/x0xx00000x

www.rsc.org/

Matthew B. Giletto,[a] Pawel A. Osmulski,[b] Corey L. Jones,[a] Maria E. Gaczynska[b]* and Jetze J. Tepe[a]*

Allosteric regulators of clinically important enzymes are gaining popularity as alternatives to competitive inhibitors. This is also the case for proteasome, a major intracellular protease and a target of anti-cancer drugs. All clinically used proteasome inhibitors bind to the active sites in catalytic chamber and display a competitive mechanism. Unfortunately, inevitable resistance associated with this type of inhibition drives the search for non-competitive agents. The multisubunit and multicatalytic "proteolytic machine" such as the proteasome is occasionally found to be affected by agents with other primary targets. For example the immunosuppressive agent rapamycin has been shown to allosterically inhibit the proteasome albeit at levels far higher than its mTOR related efficacy. As part of an ongoing program to search for novel proteasome-targeting pharmacophores, we identified the binding domain of rapamycin as required for proteasome inhibition even without the macrocyclic context of the parent compound. By subsequent structure-activity relationship studies, we generated a pipecolic ester derivative compound 3 representing a new class of proteasome inhibitors. Compound 3 affects the core proteasome activities and proliferation of cancer cells with low micromolar/high nanomolar efficacy. Molecular modeling, atomic force microscopy imaging and biochemical data suggest that compound 3 binds into one of intersubunit pockets in the proteasomal α ring and destabilizes the α face and the gate. The α face is used as a docking area for proteasome-regulating protein modules and the gate is critical for controlling access to catalytic chamber. Thus, the pipecolic ester template represents a new and attractive mechanism for proteasome inhibition distinct from classical competitive drugs.

Introduction

The proteasome is an essential protease that regulates intracellular processes and maintains biological homeostasis through the proteolytic degradation of misfolded and redundant proteins.[1] Inhibition of this essential proteasomal service induces apoptosis, a trait especially pronounced in rapidly proliferating cancer cells.[2] Not surprisingly, proteasome inhibitors became successful drugs for blood cancers, most notably multiple myeloma and mantle cell lymphoma.[3-7] All the clinically used proteasome inhibitors are small molecules designed to specifically and competitively block the major active center of this multi-catalytic protease. However, it is not uncommon for the proteasome to be affected by compounds with non-proteasomal primary targets. Notable examples include chloroquine,[8] proline and arginine (PR) rich cathelicidin PR39,[9] ritonavir,[10] chlorpromazine[11] and rapamycin.[12] Established or putative proteasome binding sites for these compounds are positioned away from catalytic centers. The consequent noncompetitive inhibition relies on allosteric mechanisms and results in diverse effects on performance of the proteasome, including changes in specificity or stability.[13] Such effects extending well beyond the activity suppression offered by the common competitive inhibitors provide an attractive opportunity to overcome the resistance to competitive drugs or to fine-tuning the physiological performance of the proteasome.[14] Thus, these unexpected secondary target compounds may provide templates for design of new proteasome regulators.[13,15] Here, we present the case of using a pharmacophore derived from rapamycin.

As we reported before, the natural product and established immunosuppressive drug rapamycin allosterically inhibits the human catalytic core of the proteasome.[12] Rapamycin and its close homologs (rapalogs) that are used as anti-cancer drugs are macrocyclic compounds sharing common "binding" and "effector" domains.[16] The former domain promotes dimerization of mTOR (mammalian/mechanistic target of rapamycin) and FKBP12 (FK-binding protein 12), whereas the latter allosterically inhibits the kinase activity of mTOR.[17,18] The mTOR signaling pathway is one of major regulators of intracellular homeostasis.[19] The anti-proteasome actions of rapamycin are exerted at much higher concentrations than the mTOR inhibition and thus would have no physiological relevance if not for some additional important observations. Namely, we found that *seco*-rapamycin, a primary metabolite and the ester hydrolysis product of rapamycin, still inhibits the proteasome while not affecting the mTOR pathway.[12] Thus, the opportunity arose to search for a novel proteasome-targeting pharmacophore.

The proteasome is a multi-subunit, multi-activity and modular enzyme. The module responsible for actual cleavage of polypeptides, the 20S core particle, is a barrel-shaped structure built

[a]Department of Chemistry, Michigan State University, East Lansing, Michigan 48824, United States
[b]Institute of Biotechnology, University of Texas Health Science Center at San Antonio, 15355 Lambda Drive, San Antonio, Texas 78245, Unites States †
Footnotes relating to the title and/or authors should appear here.
Electronic Supplementary Information (ESI) available: [details of any supplementary information available should be included here]. See DOI: 10.1039/x0xx00000x

View Article Online
DOI: 10.1039/C9OB00122K

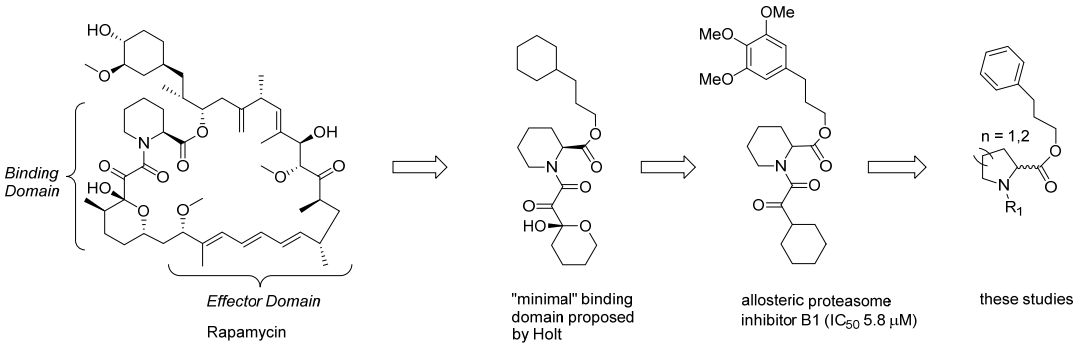

Figure 1. Design of proteasome-targeting pharmacophore of rapamycin. We found rapamycin to noncompetitively inhibit the core proteasome and traced down the putative pharmacophore to the binding domain.[11]

from four stacked pseudoheptameric rings. The inner β-rings host three pairs of active centers enclosed in a catalytic chamber and specialized in cleaving after hydrophobic or branched amino acids (the "workhorse" chymotrypsin-like activity; ChT-L), basic (trypsin-like; T-L) and acidic or small neutral amino acids (caspase-like or post-glutamyl peptide hydrolysing; PGPH).[20] The outer α-rings provide gate regulating access to the catalytic chamber and also form a binding interface ("α-face") for additional protein modules. The most common and physiologically important module is the multisubunit 19S regulatory particle that can "cap" the core and form the 26S proteasome assembly, 19S-20S-19S.[21] The core particle alone can degrade peptides and unfolded or poorly structurally organized proteins. However, at least one 19S module is required to allow the proteasome to recognize and process substrates tagged for degradation by chains of small protein ubiquitin.[22] The regulatory particle binds polyubiquitinated proteins, deubiquitinates and unfolds them, and threads into the 20S core for cleavage. The 20S proteasome exists primarily as a closed-gate (inactive) conformation in its latent form.[23-25] Conformational changes leading to gate opening can be induced by docking an activator protein onto the α-ring, by inserting the "anchors" of 19S Rpt subunits (regulatory particle ATPases) into α-ring pockets and by allosteric signaling from the active centers.[21,25-27]

Interestingly, rapamycin was found to allosterically modulate proteolytic activity by putatively binding to the α-face (the outer surface of α rings) of the 20S proteasome.[12] Since linear *seco*-rapamycin and single (binding) domain macrocycles FK506 and pimecrolimus all displayed proteasome inhibiting actions, we considered using the binding domain as a proteasome-targeting pharmacophore. We describe herein the development of small molecules with a pharmacophore resembling the "binding domain" of rapamycin, as novel scaffolds capable of allosteric regulation of the proteasome. These studies extend our earlier work on a class of **B1** compounds derived from the binding domain, which we found to inhibit the proteasome, attenuate proliferation of cultured cancer cells and suppress tumor growth in mouse xenograft models.[28]

Results and discussion

Our goal was to minimize the structure of rapamycin as a starting point for analog design. We identified the piperidine ring in the minimal domain of the parent pharmacophore (Figure 1), as an ideal starting template for functionalization. For the purpose of substrate minimization, we replaced the hemi-acetal moiety of the minimal binding domain with a cyclohexyl moiety (R_1), as we investigated the requirements of the R_2-moiety (Table 1). Prior work by Hauske illustrated the significance of the ketone as a critical recognition moiety in FKBP binding, thus our first goal was to eliminate this interaction.[29] Replacement of the ketone with a large hydrophobic substitute is known to further provide high selectivity against FKBP51, whereas smaller substituents led to loss of FKBP51 activity and binding.[30] To avoid a positive interaction with FKBP residues known to interact with either the hemiketal hydroxyl groups of FK506 or its urea's analogues,[31-34] we focused primarily on carbamate-type pipecolic acids, including benzylcarbamate as these

Scheme 1[a]

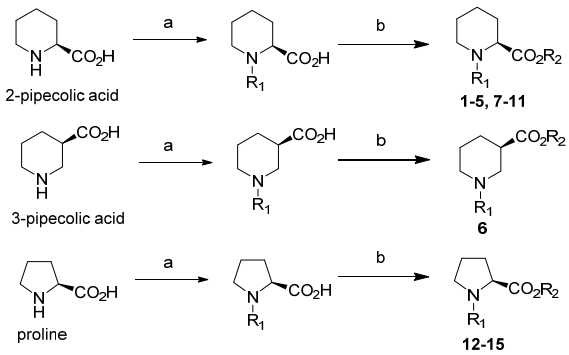

[a]Reagents and conditions: (a) R_1-Cl, Na_2CO_3, H_2O, dioxane; (b) EDCI, TEA, DMAP and R_2OH.

were previously found to be depleted of FKBP activity.[29] The compounds were prepared starting with commercially available C2- or C3- substituted pipecolic acids. Acylation of pipecolic acid with acyl chlorides or chloroformates followed by EDCI coupling of the carboxylic acid with the respective alcohols yielded products **2-11** (Scheme 1). Similarly, acylation of proline using various benzylchloroformate followed by EDCI coupling of the corresponding alcohols provided **12-15.**

We evaluated the compounds using the human housekeeping 20S proteasome. It was activated with the Rpt5 derived 10-residue peptide (KKKANLQYYA; "tail of Rpt5"; "tRpt5") that contains the C-terminal Hb-Y-X (hydrophobic-Tyr-any AA) motif activating the proteasome *in trans* and to some extent mimics the activation by the 19S regulatory particle.[12,35] Proteolytic activity was monitored

View Article Online
DOI: 10.1039/C9OB00122K

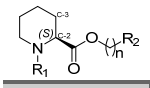	n =	R_1	R_2	CT-L IC_{50} (μM)
B1 (±)	3	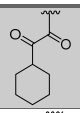	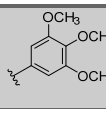	5.8
2 (±)	3		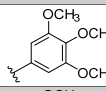	11.5
3	3		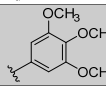	2.0
4	3		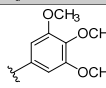	15.2
5	3		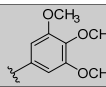	>50
6	2		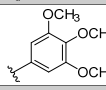	20.1
7	1		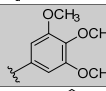	19.8
8	3			2.6
9	3		H	>50
10	0		H	>50
	3		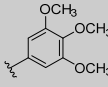	14.7
Rapamycin	NA	NA	NA	6.8

Table 1. Inhibition of ChT-L activity of tRpt5-activated 20S by pipecolic acid derivatives. Rapamycin serves as a reference.

over time using a fluorogenic peptide substrate specific for the chymotrypsin-like active center (ChT-L, Suc-LLVY-AMC) in the presence of a concentration range of the inhibitors (Tables 1 and 2). In this activity assay, hydrolysis of the substrate results in release of the highly fluorescent aminomethylcoumarin fluorophore. We used the linear portions of the fluorescence intensity plots to calculate the rates of Suc-LLVY-AMC hydrolysis and then to determine the IC_{50} (concentration of drug at which 50% of the maximum rate inhibition occurs). Starting with the R_1-moiety, we first replaced the cyclohexyl-oxoacetamide of the lead agent B1, with a benzyl carbamate to render our abridged scaffold, compound **2**. The racemate compound **2** reduced the ChT-L activity of the proteasome with an IC_{50} of 11.5 μM, which provided a good starting point to interrogate the structural requirements for activity of this new template. Next, we prepared the enantiomer of **2**, compounds (**3S**) starting from the corresponding chiral pipecolic acids. Gratifyingly, compound **3** was highly effective in reducing the ChT-L peptidase activity of the 20S with IC_{50} of 2.0 μM. Considering the stereochemical match with rapamycin and **B1**, we pursued our structure-activity relationship studies focused on the *S*-enantiomer.

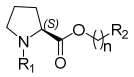	n	R_1	R_2	IC_{50} (μM)
12	3		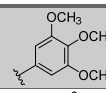	23.8
13	3		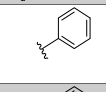	6.6
14	2		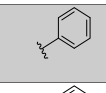	19.2
15	1	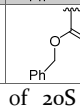	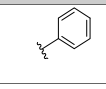	33.5

Table 2. Inhibition of 20S CT-L activity by proline derivatives.

Replacement of the benzyl carbamate with the aliphatic mimic carbamate **4**, resulted in a significant drop in activity (IC_{50} 15.2 μM). Further reduction of size (methylcarbamate **5**) completely abrogated the inhibitory effect. In addition, shortening of the R_2-chain length from n=3 to n=2 (compound **6**) or to one methylene unit (compound **7**) also significantly reduced its effectiveness. Fortunately, we found that the trimethoxy-moieties did not significantly impact the overall potency of the ester side chain and that the free aryl group (compound **8**) was found to be a potent 20S proteasome inhibitor (IC_{50} 2.6 μM). The aryl moiety did seem to be important for inhibition, since the alkyl ester **9** and carboxylic acid **10** were found to be inactive. Changes in the positioning of the ester (C-2 substitution *versus* C-3 substitution) also resulted in a drop in potency (compound **11**, IC_{50} 14.7 μM).

Next, we investigated the ring size requirements by replacing the pipecolic acid with proline. The proline analogues followed the same trends as the pipecolic acid derivatives. The proline derivative **12** only had modest activity, whereas the derivative **13** exhibited good potency (IC_{50} 6.6 μM). Reduction of the R_2-ester side chain length (compounds **14** and **15**) also decreased activity, consistent with the trend seen with the pipecolic acids **7** and **8**.

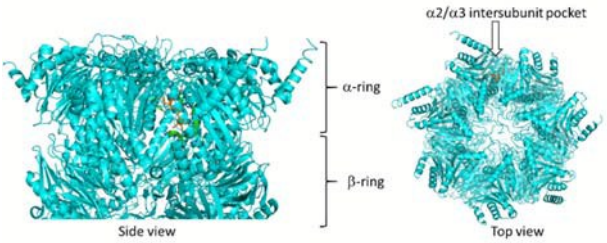

Figure 2. Docking of scaffold **3** indicates preference for binding to the α-ring on the 20S proteasome. In particular, the compound enters deep into the pocket between subunits α2 and α3. In the 26S proteasome assembly this pocket provides a binding site for the C-terminal fragment of regulatory particle ATPase Rpt6.

We conducted unbiased *in silico* docking studies to gain insight into a possible binding site of the compound in the 20S proteasome.[11] We used Autodock Vina run through PyRx to manage the workflow.[36,37] For these studies, we examined several of our most active and inactive agents. The compounds were geometry

View Article Online
DOI: 10.1039/C9OB00122K

optimized with the MM2 force field. Autodock Vina identified molecular conformations with the best fit and strongest binding affinity (global minimums). These docking studies suggest that the compounds bind into the α/α- intersubunit pockets of the α–rings, as seen with endogenous Hb-Y-X - tails of the regulatory particles (RPs or caps).[21] Compound **B1** and scaffold **3** indicated a preference for binding deep into the hydrophobic binding pocket below the α2/α3 intersubunit cavity in the α-ring (Fig. 2), The pocket is used as the binding site for the Rpt6 C-terminal "tail" of the Rpt6 subunit of the 19S regulatory particle. Compound **3** displayed preference for the α2/α3 intersubunit pockets (>0.6Kcal/mol favored over the α3/α4 and α6/α7 sites targeted), with 4 of the 9 top biding modes residing within the α2/α3 binding pocket.

Next, we tested the biochemical effects of the most potent compound **3** in more detail. The leading ChT-L activity of the 20S proteasome was not the only core peptidase affected by compound **3**. The PGPH activity was inhibited as well, with IC_{50} 2.6 μM (Fig. 3a). To the contrary, the T-L peptidase was not affected (Fig. 3a). Importantly, the activation of 20S with the tRpt5 was not mandatory to inhibit the ChT-L peptidase by compound **3**. As demonstrated in Fig. 3b, inhibition of the latent core proceeded with a respectable IC_{50} of 2.8 μM, however it plateaued at about 40% of activity left. Neither PGPH nor T-L peptidases were significantly affected, with IC_{50}>50 μM.

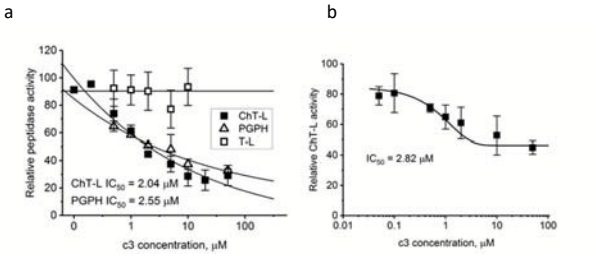

Figure 3. Compound **3** inhibits selected peptidase activities of the core 20S proteasome with low micromolar IC_{50}. (a) Not only ChT-L but also PGPH peptidase was inhibited with low-micromolar IC_{50} by the compound when the core was activated with ten-residue C-terminal peptide tRpt5 derived from the 19S ATPase Rpt5. The maximal 10-fold activation was induced by the 10 μM tRpt5, and was used in all the assays. tRpt5 was routinely added to the reaction buffer before the inhibitor. Adding compound **3** before tRpt5 did not significantly affect the proteasome response: the remaining ChT-L activity was 56% ±4% (tRpt5 last) versus 53% ±7% (tRpt5 1 first; n=3 in both cases). (b) ChT-L peptidase of the latent core was inhibited by low micromolar concentrations of compound **3**. The PGPH peptidase was not affected even by 10 μM compound 3 (99% ± 14% of control activity; n=5); only 50 μM of compound **3** reduced this activity to 71% ± 11% of the control (n=3). In turn, the T-L peptidase was weakly inhibited even at low concentrations (with 1 μM of compound 3: 77% ± 11% of the control; n=3). However, under the assay conditions, the activity was never inhibited more than 50% (with 50 μM of compound **3**: 64% ± 12%; n=4). For comparison, rapamycin inhibited the ChT-L and PGPH peptidases of the latent core with IC_{50} =1.9 μM and 0.4 μM, respectively, and activated the T-L peptidase nearly two-fold.[12]

Since the α2/α3 cavity has been demonstrated as the docking site of the C-terminal "tail" of the Rpt6 subunit of the regulatory particle,[38,39] we explored the potential competition between compound **3** and the 10-residue peptide derived from C-terminal fragment of Rpt6 (KNMSIKKLWK; tRpt6). According to the most recent model of the 26S proteasome dynamic cycle, Rpt6 succeeds the Hb-Y-X containing anchor subunits Rpt5, Rpt3 and Rpt2 in docking into the α face pockets and promoting an intermediate conformation between latent and activated (open gate) proteasomes.[39] The C-terminus of the Rpt6 subunit does not display the Hb-Y-X motif and thus it is not expected to activate the 20S core *in trans*. However, addition of the tRpt6 peptide to the 20S proteasome before addition of compound **3** significantly attenuated inhibition of the core (Fig. 4). No attenuation was observed when compound **3** was pre-incubated with the core before addition of tRpt6 (Fig. 4). Importantly, pre-incubation with tRpt6 did not affect inhibition of the proteasomal ChT-L peptidase by a competitive inhibitor, Z-LLL-VS. Namely, treatment with 0.5 μM Z-LLL-VS lowered the activity of the latent core to 54% ± 4%. The activity remained at 54% ± 6% (n=3) when the proteasome was pre-incubated with tRpt6, and at 58% ± 8% when tRpt6 was added last.

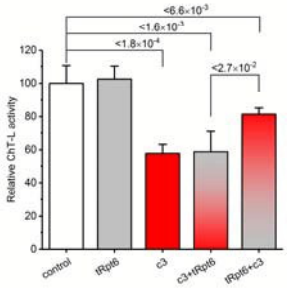

Figure 4. The C-terminal peptide derived from Rpt6 subunit compromises inhibition of the ChT-L activity of the latent core by the compound **3**, however only when added to the proteasome prior to the inhibitor. The peptide alone did not affect the proteasome activity. 1 μM compound **3** and 2 μM tRpt6 were tested. Mean ± SD; n= 3 to 6.

We interpret the result as a strong indication of competition between the tRpt6 and compound **3** for binding to the core, consistent with the outcome of *in silico* docking studies (Fig. 2). For comparison, no competition between tRpt5, expected to occupy the α5/α6 pocket, and compound **3** was detected. The tRpt5 peptide was used at the maximal-activation saturating concentration (10 μM), and the order of addition of tRpt5 and compound **3** did not compromise the inhibition (see caption to Fig. 3).

The putative binding site of compound **3** in the α ring pocket, identified by molecular modeling (Fig. 2) and biochemical data (Fig. 4), inspired us to test whether the inhibitor induced conformational changes in α face gate dynamics. For this purpose, we employed imaging of native 20S proteasomes with our established method of the atomic force microscopy (AFM). In this method, topography of the α face of buffer-submerged proteasomes that stand on their opposite α face is rendered in real time by the ultra-sharp probe. A tip of the probe interacts with the molecules mostly by van der Waals forces.[40] We routinely assess the distribution of conformation types of α face with sequential scans of fields of multiply randomly distributed proteasomes. Alternatively, we collect consecutive single scan lines representing the gate status of individual particles. We classify the particles as closed-gate if their α face is smooth and regularly concave (Fig. 5). In contrast, the open-gate particles display a centrally placed "crater". In intermediate conformers, the α face forms a slant that it is not concave and lacks a local-minimum (see Experimental section for description of numerical particle classification).[13] We found previously that the native 20S core constantly switches between these gate conformations. The abundance of conformers depends on a type of the ligand bound to the core. Namely, in the latent core in the absence of any ligands, except water molecules, the closed-gate state prevails (about

View Article Online
DOI: 10.1039/C9OB00122K

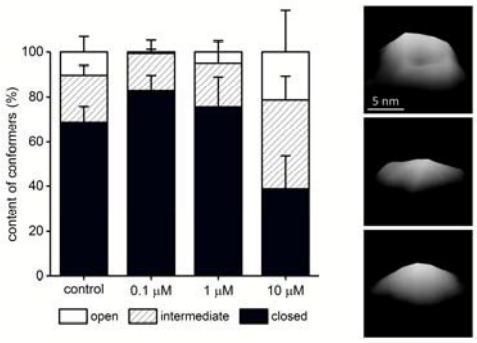

Figure 5. Compound **3** destabilizes the α face of proteasome. *Left*: The partition of conformers is shifted toward lower representation of the closed-gate particles and higher of the intermediate and open-gate 20S proteasomes upon treatment with 10 μM of compound **3**. 269 events for control and 408 events for compound **3** – treated 20S from 3 independent experiments were analysed. "Event" was a single run of the AFM probe across the proteasome particle. The differences of abundance between closed and intermediate forms were statistically significant, with p<0.0001 and p<0.0005 (T test). *Right:* AFM images (pseudo 3D, 20° tilt) of an α face of typical closed, intermediate and an open particle (top to bottom). The lighter shades of grey represent exposed (higher) portions of the α face of top-view particles.

75%).[41] Interestingly, the AFM-detected partition of closed (most stable), intermediate and open conformers in the free latent core closely matches conformational landscape of the 19S-bound core recently revealed by cryoEM studies.[42] Based on the AFM data, we proposed a model of the allosteric positive feedback loop between the active centers and the gate, with the catalytic act prompting gate opening.[25] Here, we found that presence of only 100 nM compound **3** increased the abundance of closed-gate conformers and rendered the open-gate forms nearly undetectable (Fig. 5). At 1 μM concentration of compound **3**, the open-gate proteasomes were detectable again, but their contribution was only about a half of that observed in the control particles. The landscape changed strikingly when the proteasome particles were treated with 10 μM of compound 3. Now, less than a half of the particles were in the closed-gate conformation, and the contribution of open-gate and intermediate forms increased about twice, comparing to the control (Fig. 5). We interpret this continuous decline of contribution from the closed particles in the inhibitor-treated proteasomes as a result of potential cooperativity between two identical allosteric sites being progressively saturated with compound **3**. It is plausible that the higher ligand concentrations limit coordination between the rings leading to a substantially larger representation of the intermediate conformations. Although the proteasomes still could flip between the gate conformations, their peptidolytic capabilities were severely restricted at the highest tested concentration of compound **3**. We cannot completely exclude that the weak attachment of α ring to a mica surface may limit ligand access to the binding site or change the binding site structure or constrain its dynamics effectively producing proteasomes with two binding sites of different ligand affinity. However, we did not observe such restrictions with other small ligands.[25,40] The presented results strongly indicate a destabilization α face that interferes with the allosteric network. This is not a surprising effect for the compound that likely intercalates between the α subunits (Fig. 2). Such disruption of the conformational equilibrium by allosteric regulators has been observed before. For example, treatment with cathelicidin PR39 induced a massive shift toward intermediate forms.[9] PR peptides (derivatives of PR39), imidazoline derivative TCH-165 and rapamycin all induced a strong decrease in contribution of the closed forms in the 20S particles population.[12,13,43] The activity of the core proteasome was inhibited or activated by these compounds, however a common trait was destabilization of the 26S proteasome.[12,13,43] Weakening of this most physiologically important proteasome assembly by compound **3** would be expected, as in fact it is suggested by our preliminary tests.[28]

The effects of compound **3** observed *in vitro* prompted us to test its influence on the proliferation of cultured cancer cells, namely the multiple myeloma RPMI 8226 line. The treatment did lower the content of live cells with EC_{50} of 230 nM (Fig. 6 *left*). Such relatively low EC_{50}, as compared to *in vitro* determined IC_{50} values for peptidase activities (2-3 μM; Fig. 3) should come to no surprise. Even a partial destabilization of proteasome assemblies would be

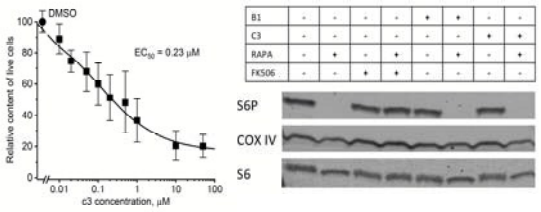

Figure 6. The compound **3** inhibits proliferation of human multiple myeloma RPMI 8226 cultured cells. However, it does not target mTOR and FKBP12, the two proteins that rapamycin is binding. *(a)* The cells were treated with compound **3** or the vehicle (DMSO) for 48 hours. The data are averages (±SD) of three-to-five independent experiments. The calculated EC_{50} based on count of live cells was 230 nM. Under the same conditions treatment with 10 nM bortezomib lowered the count to 60%±6%. *(b)* The Western blotting of extracts from RPMI 8226 cells treated for 24 hours with rapamycin (2 nM), a macrocyclic mimic of rapamycin binding domain FK506 (10 μM), compound **3** (0.2 μM) or compound B1 (0.2 μM). Under no conditions the count of live cells fell below 50% of the control. However, compound **3** and B1 inhibited the cells' proliferation to 60%-65% of control. Crude lysates prepared from the harvested cells were separated by SDS-PAGE, Western blotted and probed with specific antibodies against the mTOR substrate S6, the product of mTOR kinase PS6 (phosphorylated S6) and a "loading control" housekeeping protein COX IV. Only rapamycin inhibited phosphorylation of S6. In turn, FK506 in combination with rapamycin suppressed the inhibition by competing for binding to FKBP12. Compound **3** and B1 did not inhibit the S6 phosphorylation and did not mimic the actions of FK506. The data are representative of three independent experiments.

expected to significantly affect physiology of cancer cells. The *in vitro* readout of single peptidase activities is a useful and convenient measure of the catalytic prowess of proteasome. However, especially in the case of allosteric regulators, it may not fully reflect the important structural and functional effects. The anti-proliferative effects of compound **3** were not universal: the monocyte-like human U937 cells did not significantly respond to the treatment with 1 μM or even 10 μM compound **3**, with live cell count of 93% and 89% of vehicle-treated control, respectively (averages of two experiments differing by <10%).

Importantly, neither B1 nor compound **3** affected the activity of mTOR. As demonstrated in Fig. 6 *right*, in the cells treated with B1 or compound **3** the canonical product of mTOR kinase, phosphorylated ribosomal protein S6 (PS6) was readily detectable. Also, even if B1 and compound **3** resemble the binding domain of rapamycin, they did not emulate actions of macrocyclic binding

View Article Online
DOI: 10.1039/C9OB00122K

domain mimics such as FK506. FK506 lacks the effector domain needed for mTOR inhibition, however it binds to FKBP12. When used in excess together with rapamycin that utilizes both FKBP12 and mTOR binding, FK506 abolishes the kinase inhibition. No such actions were detectable with B1 and compound **3** used at concentrations nearing EC_{50} (Fig. 6).

Conclusions

In summary, by systematically investigating the requirements for activity of the R_1 moiety and the R_2-ester side chain, we generated a low micromolar inhibitor of the 20S proteasome (compound **3**). Molecular docking, atomic force microscopy and biochemical studies suggest that compound **3** destabilizes the α face and the gate area by inserting deep into the inter-subunit pocket in the proteasome α ring. Thus, the pipecolic ester scaffold emerges as an attractive template for a new class of allosteric proteasome inhibitors that destabilize the α ring and the gate of the core 20S proteasome, and attenuate the growth of cancer cells.

Experimental

Synthetic procedures

1-((benzyloxy)carbonyl) piperidine-2-carboxylic acid. To a 100 mL round bottom containing a stir bar was added piperidine-2-carboxylic acid (1.29 g, 10.0 mmol) followed by a water: dioxane mixture (40 mL of a 1:1 mixture). Stirring commenced and sodium carbonate was added (2.41 g, 23.0 mmol). Gas evolved; once the evolution had ceased most of the solid had dissolved. To this stirring mixture was added Cbz-Cl (1.7 mL, 2.04 g, 12.0 mmol) dropwise. The reaction mixture was allowed to stir overnight. The following day, the reaction mixture was concentrated to approximately half-volume *in vacuo*. This mixture was transferred to a separatory funnel and extracted with DCM (50 mL). This extract was discarded. In the separatory funnel, the aqueous layer was acidified by addition of concentrated HCl until the aqueous layer was acidic (pH ~ 2 by pH paper). The acidified aqueous layer was extracted 3 times with DCM (50 mL per extraction). The organic layers were combined and dried over sodium sulfate and concentrated *in vacuo* to yield the pure product as a clear oil (2.3 g, 88 %). Spectroscopic data matches that reported for this compound.(41) ^{1}H NMR (500 MHz) ($CDCl_3$) δ: 10.08 (1H, br s), 7.37 -7.31 (5H, m), 5.16 (2H, m), 5.01 – 4.90 (1H, app d), 4.10 (1H, app d), 3.10 – 2.97 (1H, m), 2.25 (1H, dd, *J* = 27.5, 12.5 Hz), 1.73 – 1.63 (3H, m), 1.47 – 1.23 (2H, m). ^{13}C NMR (125 MHz) ($CDCl_3$) δ: 177.1, 177.1, 156.8, 156.1, 136.6, 128.7, 128.6, 128.1, 127.9, 127.1 67.6, 67.5, 67.2, 54.5, 54.4, 42.0, 41.9, 26.8, 26.7, 24.8, 24.6, 20.8, 20.7.

1-benzyl 2-(3-(3,4,5-trimethoxyphenyl)propyl)piperidine-1,2-dicarboxylate (2). To a 250 mL round bottom flask containing a stir bar and 1-((benzyloxy)carbonyl)piperidine-2-carboxylic acid (5.6 g, 20.0 mmol) was added DCM (100 mL). Stirring commenced and the following reagents were added in the order listed: TEA (4.2 mL, 3.0 g, 30.0 mmol), EDCI (4.20 g, 22.0 mmol), DMAP (0.248 g, 2.0 mmol), and 3-(3,4,5-trimethoxyphenyl)propan-1-ol (4.47 g, 19.8 mmol, dissolved in 10 mL DCM). The reaction mixture was sealed with a septum, flushed with nitrogen, and allowed to proceed overnight. The following day, the reaction mixture was transferred to a separatory funnel and extracted with water. The organic layer was dried over sodium sulfate and concentrated *in vacuo* to yield the crude product. This material was purified by silica gel chromatography (1:3 ethyl acetate: hexanes, R_f = 0.22) to yield the product (>95% purity) as a clear oil (4.7 g, 50 %). ^{1}H NMR (500 MHz) ($CDCl_3$) (amide rotamers) δ: 7.35 – 7.25 (5H, m), 6.39 – 6.36 (2H, m), 5.15 – 5.10 (2H, m), 4.97 – 4.85 (1H, m), 4.17 – 4.04 (3H, m), 3.83 – 3.82 (9H, m), 3.10 – 2.94 (1H, app dt), 2.55–2.40 (2H, m), 2.25-2.20 (1H, m), 1.98 – 1.88 (2H, m), 1.71 – 1.62 (3H, m), 1.47 – 1.39 (1H, m), 1.29 – 1.21 (1H, m). ^{13}C NMR (125 MHz) ($CDCl_3$) (amide rotamers) δ: 171.6, 156.7, 153.1, 136.7, 136.5, 136.1, 128.4, 127.9, 127.7, 105.2, 67.3, 67.2, 64.2, 60.8, 56.0, 54.6, 54.4, 41.9, 32.4, 30.3, 26.7, 24.7, 24.5, 20.7, 20.6. HRMS calc'd for [M+Na] = 494.2155, observed = 494.2157.

1-((benzyloxy)carbonyl) (*S*)-piperidine-2-carboxylic acid (10). To a 100 mL round bottom containing a stir bar was added (*S*)-piperidine-2-carboxylic acid (0.500 g, 3.8 mmol) followed by a 1:1 mixture of water: dioxane (20 mL). Stirring commenced and sodium carbonate was added (0.525 g, 5.0 mmol). Gas evolved; once the evolution had ceased most of the solid had dissolved. To this stirring mixture was added Cbz-Cl (0.325 mL, 0.391 g, 2.3 mmol) dropwise. The reaction mixture was allowed to stir overnight. The following day, the reaction mixture was concentrated to approximately half-volume on a rotary evaporator. This mixture was transferred to a separatory funnel and extracted with DCM (50 mL). This extract was discarded. In the separatory funnel, the aqueous layer was acidified by addition of concentrated HCl until the aqueous layer was acidic (pH ~ 2 by pH paper). The acidified aqueous layer was extracted with DCM (3 x 50 mL). The organic layers were combined and dried over sodium sulfate and concentrated *in vacuo* to yield the product (>95% purity) as a clear oil (0.904 g, 89 %). Spectroscopic data matches that reported for this compound and the racemate.[44]

1-benzyl 2-(3-(3,4,5-trimethoxyphenyl)propyl) (*S*)-piperidine-1,2-dicarboxylate (3). To a 100 mL round bottom flask containing a stir bar was added (*S*)-2-piperidine carboxylic acid (0.250 g, 1.9 mmol), followed by a water: dioxane mixture (10 mL of a 1:1 mixture). Stirring commenced and sodium carbonate was added (0.630 g, 6.0 mmol), followed by Cbz-Cl (0.328 mL, 0.391 g, 2.3 mmol). The reaction mixture was stirred at room temperature for 48 hours. After this time, the reaction mixture was transferred to a separatory funnel and made acidic by the dropwise addition of concentrated HCl (pH ~ 2 measured by pH paper). The acidified reaction mixture was extracted with DCM (3 x 20 mL). The organic layers were combined, dried over sodium sulfate, and concentrated to dryness *in vacuo* to yield the crude product as a clear oil (0.432 g, 91 %). The crude mixture was carried on to the following step.

To a 50 mL round bottom flask containing a stir bar was added 1-benzyl 2-(3-(3,4,5-trimethoxyphenyl)propyl) (*S*)-piperidine-1,2-dicarboxylate (0.432 g, 1.7 mmol) was added DCM (10 mL) followed by TEA (0.696 mL, 0.505 g, 5.0 mmol), EDCI (0.380 g, 2.0 mmol), 3-(3,4,5-trimethoxyphenyl)propan-1-ol (0.384 g, 1.7 mmol), and DMAP (0.024 g, 0.20 mmol). The reaction vessel was sealed, flushed with nitrogen, and stirred overnight. The following day, the reaction mixture was transferred to a separatory funnel and washed with water (50 mL). The organic layer was separated, dried over sodium sulfate, and concentrated *in vacuo* to yield the product as an oil. The crude material was purified by silica gel chromatography (1:3 ethyl acetate: hexanes, R_f = 0.22) to obtain the product (>95% purity) as a clear oil (0.527 g, 66 % yield). ^{1}H NMR (500 MHz) ($CDCl_3$) (amide rotamers) δ: 7.36 – 7.30 (5H, m), 6.43 – 6.37 (2H, m), 5.16 – 5.11 (2H, m), 4.98 – 4.86 (1H, m), 4.18 – 4.05 (3H, m), 3.86 – 3.83 (9H, m), 3.12 – 2.89 (1H, m), 2.65 – 2.56 (2H, m), 2.27 – 2.12 (1H, m), 2.07 – 1.89 (2H, m), 1.72 – 1.63 (2H, m), 1.48 – 1.40 (1H, m), 1.31 – 1.22 (1H, m). ^{13}C NMR (125 MHz) ($CDCl_3$) (amide rotamers) δ: 171.6, 156 (rotamers of carbamate carbon in base-line), 153.1, 136.7, 136.5,

View Article Online
DOI: 10.1039/C9OB00122K

136.2, 128.4, 128.0, 127.7, 105.2, 67.3, 67.2, 64.3, 64.2, 60.8, 56.0, 54.7, 54.4, 41.9, 32.4, 30.3, 30.2, 26.7, 24.7, 24.5, 20.7, 20.6. HRMS calc'd for [M+H] = 472.2335, observed = 472.2333.

1-(isobutoxycarbonyl) (*S*)-piperidine-2-carboxylic acid. To a 50 mL round bottom flask containing a stir bar was added (*S*)-pipecolic acid (0.250 g, 1.9 mmol) and water (5 mL) followed by 2N aqueous sodium hydroxide (0.200 g, 5.0 mmol in 5 mL water). Stirring commenced and isobutyl chloroformate was added (0.275 mL, 0.285 g, 2.1 mmol). The reaction mixture was allowed to stir overnight. The following day, the reaction was quenched by the addition of concentrated HCl (until the mixture was pH ~ 2 by pH paper) and extracted with ethyl acetate (2 x 25 mL). The organic layers were combined, dried over sodium sulfate, and concentrated *in vacuo* to yield the crude product as an oil. The crude material was purified by filtering through a plug of silica gel (1:2 ethyl acetate: hexanes) to yield the pure product as a clear oil which solidifies on standing (0.302 g, 69 %). ^{1}H NMR (500 MHz) ($CDCl_3$) (amide rotamers) δ: 10.31 (1H, br s), 4.91 (1H, br d), 4.05 (1H, br d), 3.92 – 3.82 (2H, m), 3.07 – 2.95 (1H, m), 2.25 (1H, br t, *J* = 14.0 Hz), 1.98 – 1.90 (1H, m), 1.74 – 1.65 (3H, m), 1.46 – 1.40 (1H, m), 1.36 – 1.28 (1H, m), 0.92 (6H, dd, *J* = 21.0, 7.0 Hz). ^{13}C NMR (125 MHz) ($CDCl_3$) (amide rotamers) δ: 177.7, 177.5, 156.9, 156.2, 71.9, 71.8, 54.2, 54.0, 41.7, 41.5, 27.9, 26.7, 26.5, 24.6, 24.4, 20.7, 20.6, 19.0. HRMS calc'd for [M – H] = 228.1241, observed = 228.1233. IR (NaCl, DCM): 3095, 2960, 2874, 1744, 1704, 1667, 1470. M.P. = 67 ºC.

1-isobutyl 2-(3-(3,4,5-trimethoxyphenyl)propyl) (*S*)-piperidine-1,2-dicarboxylate (4). To a 100 mL round bottom flask containing a stir bar was added 1-(isobutoxycarbonyl)piperidine-2-carboxylic acid (0.302 g, 1.32 mmol) followed by DCM (10 mL). To this solution was added 3-(3,4,5-trimethoxyphenyl)propan-1-ol (0.316 g, 1.4 mmol dissolved in 2 mL DCM). Stirring commenced and the following reagents were added in the order listed: EDCI (0.304 g, 1.6 mmol), TEA (0.350 mL, 0.252 g, 2.5 mmol) and DMAP (0.06 g, 0.50 mmol). The reaction vessel was sealed, flushed with nitrogen, and allowed to stir overnight. The following day, the reaction mixture was transferred to a separatory funnel and washed with water (50 mL). The organic layer was dried with sodium sulfate and concentrated *in vacuo* to yield the crude product as an oil. This material was purified by silica gel chromatography (1:3 ethyl acetate: hexanes, R_f = 0.32) to yield the product (>95% purity) as a clear oil (0.301 g, 52 % yield). ^{1}H NMR (500 MHz) ($CDCl_3$) (amide rotamers) δ: 6.39 (2H, s), 4.95 – 4.83 (1H, br d), 4.17 – 3.91 (4H, m), 3.90 – 3.82 (9 H, m), 3.09 – 2.93 (1H, br dt), 2.62 (2H, br t, *J* = 7.0 Hz), 2.25 – 2.22 (1H, m), 1.99 – 1.89 (3H, m), 1.74 – 1.64 (4H, m), 1.45 – 1.43 (1H, m), 1.30 – 1.22 (1H, m), 0.94 – 0.88 (6H, m). ^{13}C NMR (125 MHz) ($CDCl_3$) (amide rotamers) δ: 171.8, 171.8, 156.8, 156.2, 153.1, 136.7, 136.2, 105.2, 71.7, 71.6, 64.3, 64.2, 60.8, 56.0, 54.5, 54.3, 41.7, 32.4, 30.3, 30.3, 27.9, 26.8, 26.7, 24.7, 24.5, 20.8, 20.6, 19.0. HRMS calc'd for [M+H] = 438.2492, observed = 438.2494.

1-(methoxycarbonyl) (*S*)-piperidine-2-carboxylic acid. To a 50 mL round bottom flask containing a stir bar was added (*S*)-pipecolic acid (0.250 g, 1.9 mmol) and water (5 mL) followed by 2N aqueous sodium hydroxide (0.200 g, 5.0 mmol in 5 mL water). Stirring commenced and methyl chloroformate was added (0.160 mL, 0.198 g, 2.1 mmol). The reaction mixture was allowed to stir overnight. The following day the reaction was quenched with the addition of concentrated HCl (until pH ~ 2 by pH paper) and extracted twice with ethyl acetate (30 mL per extraction). The organic layers were dried over sodium sulfate and concentrated to dryness *in vacuo* to yield the crude product as a clear oil. The crude material was purified by silica gel chromatography (1:1 ethyl acetate: hexanes) to yield the pure produce as a clear oil (0.238 g, 66 %). Spectroscopic data matches that reported for this compound.[45] ^{1}H NMR (500 MHz) ($CDCl_3$) (amide rotamers) δ: 9.65 (1H, br s), 4.90 (1H, app d), 4.04 (1H, app dd), 3.72 (3H, app d), 3.06 – 2.94 (1H, m), 2.25 (1H, br t, *J* = 15.0 Hz), 1.73 – 1.64 (3H, m), 1.44 – 1.27 (2H, m). ^{13}C NMR (125 MHz) ($CDCl_3$) (amide rotamers): 177.5, 177.4, 157.3, 156.6, 54.3, 54.0, 53.0, 41.8, 41.6, 26.7, 26.5, 24.6, 24.4, 20.6.

1-methyl 2-(3-(3,4,5-trimethoxyphenyl)propyl) (*S*)-piperidine-1,2-dicarboxylate (5). To a 50 mL round bottom flask was added 1-(methoxycarbonyl) (*S*)-piperidine-2-carboxylic acid (0.238 g, 1.32 mmol) followed by DCM (10 mL). Stirring commenced and to the reaction mixture was added the following (in the order listed): EDCI (0.304 g, 1.6 mmol) and DMAP (0.060 g, 0.5 mmol). The reaction vessel was sealed with a septa and flushed with nitrogen. To the stirring reaction mixture was added via syringe (in the order listed): TEA (0.350 mL, 0.252 g, 2.5 mmol) followed by 3-(3,4,5-trimethoxyphenyl)propan-1-ol (0.293 g, 1.3 mmol dissolved in 3.0 mL DCM). The reaction mixture was allowed to stir overnight. The following day, the reaction was quenched by the addition of water (10 mL) and partitioned in a separatory funnel. The organic layer was dried over sodium sulfate and concentrated to dryness *in vacuo* to yield the crude product as an oil. The crude material was purified by silica gel chromatography (1:2 ethyl acetate: hexanes, R_f = 0.42) to yield the product (>95% purity) as a clear oil (0.222 g, 44 %). ^{1}H NMR (500 MHz) ($CDCl_3$) (amide rotamers) δ: 6.39 (2H, s), 4.95 – 4.80 (1H, m), 4.17 – 4.11 (2H, m), 3.87 – 3.82 (9H, m), 3.72 – 3.70 (3H, m), 3.08 – 2.92 (1H, m), 2.62 (2H, br t, *J* = 7.0 Hz), 2.25 – 2.23 (1H, m), 1.96 (2H, quintet, *J* = 7.0 Hz), 1.72 – 1.63 (4H, m), 1.44 – 1.42 (1H, br m), 1.29 – 1.21 (1H, m). ^{13}C NMR (125 MHz) ($CDCl_3$): δ: 171.7, 157.2 and 156.56 (carbamate rotamers), 153.2, 136.7, 136.2, 105.2, 64.2, 60.8, 56.0, 54.3, 52.8, 41.8, 32.4, 30.3, 26.7, 24.7, 24.5, 20.7. HRMS calc'd for [M+H] = 396.2022, observed = 396.2019.

(*R*)-1-((benzyloxy)carbonyl)piperidine-3-carboxylic acid. To a 100 mL round bottom flask containing a stir bar was added (*R*)-3-pipecolic acid (1.0 g, 7.7 mmol) followed by 1,4-dioxane (10 mL) and water (10 mL). Stirring commenced and sodium carbonate was added (2.1 g, 20.0 mmol) followed by Cbz-Cl (1.20 mL, 1.44 g, 8.5 mmol). The reaction mixture was stirred overnight. The following day the reaction was quenched by the addition of HCl (36 mmol HCl 10 mL of a 3.6 M solution). The reaction mixture was transferred to a separatory funnel and extracted with ethyl acetate (3 x 20 mL per extraction). The organic layers were combined, dried over sodium sulfate, and concentrated *in vacuo* to yield the crude product as an oil. This material was dissolved in a 1:1 mixture of ethyl acetate: hexanes and passed through a plug of silica gel to yield the crude product as an oil that on standing turns into a waxy, white solid (1.74 g, 84 %). ^{1}H NMR (500 MHz) ($CDCl_3$) (amide rotamers) δ: 7.38 – 7.29 (5H, m), 5.17 – 5.10 (2H, m), 4.27 – 4.15 (1H, m), 3.97 (1H, dt, *J* = 9.5, 3.5, 3.5 Hz), 3.17 – 3.06 (1H, m), 2.96 – 2.90 (1H, m), 2.51 (1H, br s), 2.10 – 2.07 (1H, m), 1.74 – 1.65 (2H, m) 1.50 (1H, br s). ^{13}C NMR (125 MHz) ($CDCl_3$) (amide rotamers): 178.8, 155.2, 136.6, 128.5, 128.0, 127.9, 67.2, 45.4, 44.1, 40.9, 27.0, 24.0. HRMS calc'd for [M+H] = 264. 1236, observed = 264.1259; calc'd for [M+Na] = 286. 1055, observed = 286. 1058. M.P. = 97 ºC.

1-benzyl 2-(3,4,5-trimethoxyphenethyl) (*S*)-piperidine-1,2-dicarboxylate (6). To a 500 mL round bottom flask containing a stir

View Article Online
DOI: 10.1039/C9OB00122K

bar and (*S*)-1-((benzyloxy)carbonyl)piperidine-2-carboxylic acid (0.386 g, 1.5 mmol) was added DCM (10 mL). Stirring commenced, and in the order listed was added TEA (0.417 mL, 0.303 g, 3.0 mmol), EDCI (0.323 g, 1.7 mmol), DMAP (0.060 g, 0.50 mmol), and 2-(3,4,5-trimethoxyphenyl)ethan-1-ol (0.318 g, 1.5 mmol). The reaction vessel was sealed, flushed with nitrogen, and allowed to stir overnight. The following day, the reaction mixture was quenched with water (10 mL) and partitioned in a separatory funnel. The organic layer was dried over sodium sulfate and concentrated *in vacuo* to a yellow oil. The crude product was purified by silica gel chromatography (1:3 ethyl acetate: hexanes) to yield the product (>95% purity) as a clear oil (0.145 g, 21 %). ^{1}H NMR (500 MHz) ($CDCl_3$) (amide rotamers) δ: 7.37 – 7.29 (5H, m), 6.41 (2H, d, *J* = 14.0 Hz), 5.16 – 5.10 (2H, m), 4.95 – 4.82 (1H, m), 4.38 – 4.29 (2H, m), 4.09 – 3.99 (1H, m), 3.84 (6H, app d, *J* = 3.5 Hz), 3.81 (3H, app d, *J* = 5.0 Hz), 3.00 – 2.80 (3H, m), 2.17 (1H, t, *J* = 16.0 Hz), 1.67 – 1.56 (3H, m), 1.43 – 1.38 (1H, m), 1.55 – 1.10 (1H, m). ^{13}C NMR (125 MHz) ($CDCl_3$) (amide rotamers) δ: 171.6, 171.6, 156.5, 155.9, 153.2, 136.6, 136.6, 133.2, 133.1, 128.4, 128.0, 127.8, 105.7, 67.3, 67.1, 65.5, 65.4, 60.8, 56.0, 54.6, 54.4, 41.8, 41.7, 35.4, 35.3, 26.7, 24.6, 24.4, 20.6, 20.5. HRMS calc'd for [M+Na] = 480.1998, observed = 480.2011.

1-benzyl 2-(3,4,5-trimethoxybenzyl) piperidine-1,2-dicarboxylate (7). To a 100 mL round bottom flask containing a stir bar was added 1-((benzyloxy)carbonyl)piperidine-2-carboxylic acid (0.435 g, 1.6 mmol), followed by DCM 1 mL). The reaction mixture was stirred and the following reagents were added (in the order listed): TEA (0.417 mL, 0.303 g, 3.0 mmol), EDCI (0.342 g, 1.8 mmol), and DMAP (0.060 g, 0.50 mmol). Stirring commenced and the reaction vessel was sealed with a septa and flushed with nitrogen. To this mixture was added 3,4,5-trimethoxybenzyl alcohol (0.273 mL, 0.336 g, 1.7 mmol, dissolved in 2.0 mL DCM) via syringe. The reaction mixture was allowed to stir overnight. The following day, the reaction mixture was transferred to a separatory funnel and extracted with water (50 mL) and brine (50 mL). The organic layer was dried over sodium sulfate and concentrated *in vacuo* to yield the crude product as a clear oil. The crude material was purified by silica gel chromatography (1:3 ethyl acetate: hexanes, R_f = 0.28) to yield the final product (>95% purity) as a clear oil (0.371 g, 50 %). ^{1}H NMR (500 MHz) ($CDCl_3$) (amide rotamers) δ: 7.35 – 7.25 (5H, m), 6.55 – 6.52 (2H, m), 5.15 – 4.89 (5H, m), 4.14 – 4.03 (1H, m), 3.83 – 3.82 (9H, m), 3.11 – 2.96 (1H, m), 2.28 – 2.21 (1H, m), 1.70 – 1.41 (4H, m), 1.28 – 1.22 (1H, m). ^{13}C NMR (125 MHz) ($CDCl_3$) (amide rotamers) δ: 171.5, 156.4, 155.9, 153.3, 137.7, 136.5, 131.4, 131.2, 128.4, 128.4, 128.0, 127.7, 127.6, 104.9, 104.8, 67.3, 67.2, 66.8, 60.8, 56.1, 54.7, 54.4, 41.9, 41.8, 26.7, 24.7, 24.5, 20.7, 20.6. HRMS calc'd for [M+Na] = 466.1842, observed = 466.1845.

1-benzyl 2-(3-phenylpropyl) (*S*)-piperidine-1,2-dicarboxylate (8). To a 50 mL round bottom flask containing a stir bar was added 1-((benzyloxy)carbonyl) (*S*)-piperidine-2-carboxylic acid (0.523 g, 1.98 mmol), followed by DCM (20 mL). To the reaction vessel was added (in the order listed) EDCI (0.45 g, 2.5 mmol), TEA (0.696 mL, 0.505 g, 5.0 mmol), and DMAP (0.060 g, 0.50 mmol). The reaction vessel was sealed and flushed with nitrogen. Stirring commenced and 3-phenyl-1-propanol was added via syringe (0.258 mL, 0.258 g, 1.9 mmol). The reaction was allowed to proceed overnight. The following day, the reaction was transferred to a separatory funnel in which it was washed with water (10 mL), dilute HCl (10 mL 0.5 M HCl), saturated aqueous sodium bicarbonate (20 mL) and brine. The crude product was dried over sodium sulfate and concentrated to dryness *in vacuo*. The crude product was purified by silica gel chromatography (1:4 ethyl acetate: hexanes, R_f = 0.30) to yield the product (>95% purity) as a clear oil (0.276 g, 38 %). ^{1}H NMR (500 MHz) ($CDCl_3$) (amide rotamers) δ: 7.35 – 7.13 (10H, m), 5.16 – 5.13 (2H, m), 4.97 – 4.85 (1H, m), 4.15 – 4.05 (3H, m), 3.10 – 2.94 (1H, m), 2.68 – 2.61 (2H, m), 2.27 – 2.19 (1H, m), 1.98 – 1.89 (2H, m), 1.71 – 1.62 (3H, m), 1.47 – 1.41 (1H, m), 1.29 – 1.21 (1H, m). ^{13}C NMR (125 MHz) ($CDCl_3$) (amide rotamers) δ: 171.6, 156.5, 155.4, 141.0, 136.6, 128.4, 128.4, 127.9, 127.8, 126.0, 67.3, 67.2, 64.3, 54.6, 54.4, 41.9, 41.8, 32.0, 30.0, 26.8, 26.7, 24.7, 24.5, 20.7, 20.6. HRMS calc'd for [M+H] = 382.2018, observed = 382.2044.

1-benzyl 2-propyl (*S*)-piperidine-1,2-dicarboxylate (9). To a 50 mL round bottom flask containing a stir bar was added (*S*)-2-(propoxycarbonyl)piperidin-1-ium chloride (0.220 g, 1.06 mmol) followed by dioxane (2 mL) and water (2 mL). Stirring commenced and sodium carbonate was added as a solid (0.315 g, 3.0 mmol), followed by Cbz-Cl (0.170 mL, 0.204 g, 1.2 mmol). The reaction mixture was stirred at room temperature overnight. The following day the reaction was quenched by the addition of HCl (24.0 mmol, 2 mL conc. HCl and 8 mL distilled water). The reaction mixture was transferred to a separatory funnel and extracted with ethyl acetate (3 x 15 mL per extraction). The crude material was concentrated *in vacuo* to yield an oil, which was purified by silica gel chromatography (1:2 ethyl acetate: hexanes) to yield the product (>95% purity) as a clear oil (0.266 g, 75 %). ^{1}H NMR (500 MHz) ($CDCl_3$) (amide rotamers) δ: 7.36 – 7.30 (5H, m), 5.17 – 5.09 (2H, m), 4.95 – 4.83 (1H, m), 4.13 – 4.03 (3H, m), 3.10 – 2.94 (1H, m), 2.27 – 2.19 (1H, m), 1.70 – 1.58 (5H, m), 1.46 – 1.40 (1H, m), 1.29 – 1.21 (1H, m), 0.94 – 0.88 (3H, m). ^{13}C NMR (125 MHz) ($CDCl_3$) (amide rotamers): 171.7, 171.6, 156.5, 155.9, 136.6, 128.5, 128.4, 127.9, 127.7, 67.2, 67.1, 66.6, 54.6, 54.4, 41.8, 41.8, 26.8, 26.7, 24.7, 24.5, 21.9, 20.7, 20.6, 10.4. HRMS calc'd for [M+H] = 306.1705, observed = 306.1708.

1-benzyl 3-(3-(3,4,5-trimethoxyphenyl)propyl) (*R*)-piperidine-1,3-dicarboxylate (11). To a 100 mL round bottom flask containing (*R*)-1-((benzyloxy)carbonyl)piperidine-3-carboxylic acid (0.542 g, 2.0 mmol) was added a stir bar followed by DCM (15 mL), EDCI (0.414 g, 2.2 mmol), TEA (0.696 mL, 0.505 g, 5.0 mmol), DMAP (0.060 g, 0.5 mmol), and 3-(3,4,5-trimethoxyphenyl)propan-1-ol (0.461 g, 2.0 mmol). The reaction mixture was stirred overnight. The reaction mixture was transferred to a separatory funnel and washed with dilute HCl (10 mL 5 % HCl v/v) followed by saturated aqueous sodium bicarbonate (20 mL). The organic layer was dried over sodium sulfate and concentrated *in vacuo*. The crude material was purified by silica gel chromatography (1:2 ethyl acetate: hexanes) to yield the product (>95% purity) as a clear oil (0.453 g, 48 %). ^{1}H NMR (500 MHz) ($CDCl_3$) (amide rotamers) δ: 7.36 – 7.30 (5H, m), 6.39 (2H, s), 5.16 – 5.11 (2H, m), 4.28 – 3.90 (4H, m), 3.84 – 3.82 (9H, m), 3.15 – 3.04 (1H, m), 2.95 – 2.90 (1H, m), 2.62 (2H, br t, *J* = 7.0 Hz), 2.50-2.48 (1H, bm), 2.08 – 2.05 (1H, m), 1.97 – 1.92 (2H, m), 1.72 – 1.62 (2H, m), 1.50 (1H, br s). ^{13}C NMR (125 MHz) ($CDCl_3$) (amide rotamers): 173.2, 155.1, 153.1, 136.8, 136.7, 136.2, 128.5, 128.0, 127.8, 105.2, 67.1, 63.9, 60.8, 56.0, 45.7, 44.2, 41.3, 32.5, 30.2, 27.2, 24.3. HRMS calc'd for [M+H] = 472.2335, observed = 472.2331.

1-benzyl 2-(3-(3,4,5-trimethoxyphenyl)propyl) (*S*)-pyrrolidine-1,2-dicarboxylate (12). To a 100 mL round bottom flask containing ((benzyloxy)carbonyl)-*L*-proline (1.59 g, 6.4 mmol) was added a stir bar and DCM (50 mL). The reaction mixture was stirred and the following reagents were added in the order listed: EDCI (1.33 g, 7.0 mmol), DMAP (0.122 g, 1.0 mmol), and TEA (1.01 g, 10.0 mmol). The reaction vessel was sealed and flushed with nitrogen. To the stirring

View Article Online
DOI: 10.1039/C9OB00122K

mixture was added 3-(3,4,5-trimethoxyphenyl)propan-1-ol (1.44 g, 6.4 mmol) via syringe dissolved in DCM (10 mL). The reaction was allowed to stir overnight. The following day, the reaction was quenched with water (50 mL), transferred to a separatory funnel and partitioned. The organic layer was dried over sodium sulfate and concentrated *in vacuo*. The crude material was purified by silica gel chromatography (1:3 ethyl acetate: hexanes, R_f = 0.51) to yield the product (>95% purity) as a clear oil (1.3 g, 42 % yield). ^{1}H NMR (500 MHz) ($CDCl_3$) (amide rotamers) δ: 7.36 – 7.24 (5H, m), 6.39 – 6.34 (2H, app d), 5.19 – 5.06 (2H, m), 4.38 (1H, ddd, *J* = 19.5, 15.5, 3.5 Hz), 4.19 – 4.00 (2H, m), 3.84 – 3.80 (9H, m), 3.66 – 3.47 (2H, m), 2.62 (1H, t, *J* = 7.5 Hz), 2.51 (1H, t, *J* = 8.0 Hz), 2.28 – 2.20 (1H, m), 2.02 – 1.80 (5H, m). ^{13}C NMR (125 MHz) ($CDCl_3$) (amide rotamers) δ: 172.8, 172.7, 154.8, 154.2, 153.1, 153.1, 136.9, 136.7, 136.6, 136.5, 136.1, 136.1, 128.4, 128.3, 127.9, 127.8, 127.7, 105.2, 105.1, 66.9, 66.9, 64.3, 64.2, 60.8, 59.3, 58.9, 56.0, 46.9, 46.4, 32.3, 32.3, 31.0, 30.3, 30.1, 29.9, 24.3, 23.5. HRMS calc'd for [M+H] = 458.2179, observed = 458.2177.

1-benzyl 2-(3-phenylpropyl) (*S*)-pyrrolidine-1,2-dicarboxylate (13). To a 250 mL oven dried round bottom flask containing a stir bar was added ((benzyloxy)carbonyl)-*L*-proline (2.50 g, 10.0 mmol), followed by DCM (100 mL). Stirring commenced, and to the reaction mixture was added (in the order listed) TEA (1.7 mL, 1.21 g, 12.0 mmol), EDCI (2.0 g, 11.0 mmol), DMAP (0.244 g, 0.2 mmol), and 3-phenyl-1-propanol (1.49 g, 1.49 mL, 11.0 mmol). The reaction vessel was sealed and flushed with nitrogen and allowed to react overnight. The following day, the reaction mixture was transferred to a separatory funnel and extracted with water (once, 100 mL). The crude reaction mixture was concentrated on a rotary evaporator and purified through silica gel chromatography (1:4 ethyl acetate: hexanes, R_f = 0.33) to yield the product (>95% purity) as a clear oil (2.1 g, 57 %). ^{1}H NMR (500 MHz) ($CDCl_3$) (amide rotamers) δ: 7.39 – 7.12 (10H, m), 5.20 – 5.07 (2H, m), 4.43 – 4.34 (1H, m), 4.19 – 4.14 (1H, m), 4.07 – 3.97 (1H, m), 3.70 – 3.45 (2H, m), 2.74 – 2.67 (1H, m), 2.58 (1H, t, *J* = 7.5 Hz), 2.30 – 2.18 (1H, m), 2.03 – 1.81 (5H, m). ^{13}C NMR (125 MHz) ($CDCl_3$) (amide rotamers) δ: 172.8, 172.6, 154.3, 141.1, 140.9, 136.7, 136.5, 128.5, 128.4, 128.4, 128.3, 128.3, 127.9, 127.9, 127.8, 127.8, 126.0, 126.0, 125.8, 67.0, 66.9, 64.3, 64.3, 62.3, 59.3, 58.9, 46.9, 46.4, 34.2, 32.0, 32.0, 31.9, 30.9, 30.2, 30.0, 29.9, 29.8, 26.8, 24.3, 23.5. HRMS calc'd for [M+H] = 368.1826, observed = 368.1862.

1-benzyl 2-phenethyl (*S*)-pyrrolidine-1,2-dicarboxylate (14). To a 100 mL round bottom flask containing a stir bar and ((benzyloxy)carbonyl)-*L*-proline (2.3 g, 9.2 mmol) was added DCM (50 mL). Stirring commenced and the following reagents were added (in the order listed) EDCI (2.18, 11.5 mmol), TEA (2.52 mL, 2.02 g, 20.0 mmol), DMAP (0.120 g, 0.1 mmol) and 2-phenylethanol (0.976 mL, 0.976 g, 8.0 mmol). The reaction vessel was sealed with a septa and flushed with nitrogen. Stirring commenced and the reaction was allowed to proceed overnight. The following day, the reaction mixture was transferred to a separatory funnel and washed with water (50 mL) and brine (50 mL). The crude material was concentrated *in vacuo* to yield an oil which was dissolved in a minimum amount of DCM and purified by silica gel chromatography (gradient 1:9 to 1:4 ethyl acetate: hexanes) to yield the product (>95% purity) as a clear oil (0.985 g, 33 %). ^{1}H NMR (500 MHz) ($CDCl_3$) (amide rotamers) δ 7.43 – 7.05 (m, 10H), 5.29 – 4.91 (m, 3H) (should be 2H, extra integration 1H likely DCM solvent), 4.45 – 4.29 (m, 2H), 4.22 (m, 1H), 3.68 – 3.42 (m, 2H), 2.95 (t, J = 7.1 Hz, 1H), 2.81 (t, J = 7.0 Hz, 1H), 2.19 (m, 1H), 1.96 – 1.78 (m, 3H). ^{13}C NMR (125 MHz) ($CDCl_3$) (amide rotamers): 172.7, 172.5, 154.8, 154.2, 137.6, 137.4, 136.7, 136.6, 128.9, 128.8, 128.5, 128.4, 128.4, 128.4, 128.3, 128.2, 128.1, 128.0, 127.9, 127.9, 127.8, 127.8, 127.8, 126.6, 126.5, 67.0, 66.9, 66.9, 66.9, 66.8, 66.7, 65.4, 65.3, 59.2, 58.9, 46.9, 46.9, 46.4, 46.3, 35.0, 34.8, 30.9, 29.8, 24.3, 24.2, 23.5, 23.4. HRMS calc'd for [M+Na] = 376.1525, observed = 376.1525.

dibenzyl (*S*)-pyrrolidine-1,2-dicarboxylate (15). To a 100 mL round bottom flask containing a stir bar was added benzyl-*L*-prolinate (purchased from Alfa Aesar, 0.858 g, 4.4 mmol) followed by DCM (20 mL). The vessel was sealed with a septa and flushed with nitrogen. To the stirring reaction mixture was added TEA (0.835 mL, 0.606 g, 6.0 mmol) and Cbz-Cl (0.580 mL, 0.697 g, 4.1 mmol). The reaction mixture was allowed to stir overnight. The following day the reaction mixture was transferred to a separatory funnel and extracted with dilute HCl (20 mL of 5 % HCl v/v) and saturated sodium bicarbonate solution (20 mL). The organic layer was dried over sodium sulfate and concentrated *in vacuo* to yield the crude product. The crude material was purified by silica gel chromatography (1:2 ethyl acetate: hexanes, R_f = 0.4) to yield the product (>95% purity) as a clear oil (0.724 g, 51 %). ^{1}H NMR (500 MHz) ($CDCl_3$) (amide rotamers) δ: 7.38 – 7.23 (10H, m), 5.24 – 5.12 (2H, m), 5.09 – 5.00 (2H, m), 4.48 – 4.38 (1H, m), 3.67 – 3.57 (1H, m), 3.55 – 3.46 (1H, m), 2.29 – 2.19 (1H, m), 2.05 – 1.86 (3H, m). ^{13}C NMR (125 MHz) (500 MHz) ($CDCl_3$) (amide rotamers) δ: 172.6, 172.4, 154.9, 154.2, 136.7, 136.5, 135.7, 135.5, 128.5, 128.4, 128.4, 128.3, 128.2, 128.1, 128.0, 127.9, 127.9, 127.8, 127.7, 67.0, 66.9, 66.8, 66.7, 59.2, 58.9, 46.9, 46.4, 30.9, 29.9, 24.3, 23.5. HRMS for [M+H] = 340.1549, observed = 340.1549.

Determination of proteasome activity. Human housekeeping 20S purified from erythrocytes was purchased from Enzo Life Sciences, Inc. (Farmingdale, NY) or from Boston Biochem, Inc. (Cambridge, MA) The 1 mg/ml stock 20S proteasome was diluted to 0.2 mg/ml working solution in 50 mM Tris/HCl, pH 8 containing 20% glycerol (dilution buffer). The peptidase activities were measured as arbitrary intensity units of fluorescence emitted by 7-amino-4-methylcoumarin (AMC) released from the canonical model peptide substrates: succinyl-LeuLeuValTyr-AMC (for the ChT-L peptidase; SucLLVY-AMC; Bachem Bioscience Inc., Philadelphia, PA), butoxycarbonyl-LeuArgArg-AMC (T-L; Bachem Bioscience Inc., Philadelphia, PA) and carbobenzoxy- LeuLeuGlu-AMC (PGPH; Enzo Life Sciences Inc., Farmingdale, NY), all used at concentration of 100 µM. Free AMC (Sigma-Aldrich, St. Louis, MO) was used as the standard. The tRpt5 and tRpt6 C-terminal peptides were synthesized (standard solid-phase peptide chemistry) and purified to at least 98% purity by GenScript (Piscataway, NJ). The tRpt5 peptide and the peptide substrates were dissolved in anhydrous dimethylsulfoxide (DMSO; Sigma-Aldrich, St. Louis, MO) and such stock solutions were stored at -20oC. The total concentration of DMSO in final reaction mixtures never exceeded 3% (vol/vol). The Trp-containing tRpt6 peptide was dissolved in ultrapure water and stored at -20°C, protected from light. The reaction was carried out in 96-well plates, in 100 µL of reaction mixture, for 1 hour at 37°C, with fluorescence readout once per minute.[12] The reaction mixture consisted of 45 mM Tris/HCl, pH 8, 100 mM KCl, 1 mM EDTA (reaction buffer) and 100 µM of a fluorogenic peptide substrate, to which 200 ng (nearly 0.3 nmol) of proteasome and desired concentration of tested compounds in 0.5 µL of DMSO were added. If desired, the proteasome was activated with 10 µM (final concentration) of the tRpt5 peptide premixed in the reaction mixture. To test the competition with tRpt6 peptide the 20S proteasome was pre-

View Article Online
DOI: 10.1039/C9OB00122K

incubated in the reaction buffer for 10 min (RT) with compound **3** or carbobenzoxy-LeuLeuLeu-vinyl sulfone (Z-LLL-VS; Enzo Life Sciences, Inc), or tRpt6, or solvents, and then the compounds/solvents and the substrate were added, as indicated. The reaction rates were calculated from a linear segment of kinetic curves constructed from measurements in 1-minutes intervals (Fluoroskan Ascent plate reader; Thermo Fisher Scientific Inc., Waltham, MA). Reaction rates were calculated using a linear fit performed with the Slope Analyser and Enzyme Kinetics applications launched within Origin Pro 2017 (OriginLab Corporation, Northampton, MA). Specific activity of the control 20S proteasome activated with the Rpt5 peptide was in the range of 1.4 to 2.3 nanomoles of AMC product released by 1 mg of 20S per second (1.95 ± 0.24; n=18). The activity of a latent proteasome (no tRpt5 added) was 7 to 10 times lower. The data are presented as mean ± SD or as a representative set from at least 3 independent experiments.

Atomic force microscopy (AFM) imaging. The single molecule imaging of the 20S proteasome was carried out as previously described, with a scanner E of the Multimode Nanoscope IIIa (Bruker Inc).[13,25] In short, the proteasomes were deposited and electrostatically attached to a muscovite mica substrate, covered with imaging buffer (5 mM Tris/HCl, pH 7) and scanned in tapping mode in fluid using cantilevers with the spring constant of 0.35 N/m from the SNL (Sharp Nitride Lever) probes (Bruker Inc.) tuned to 9 – 10 kHz. Gentle scanning conditions with the amplitude set-point in the range of 1.5 - 2.0V, drive voltage of 300-500 mV and 3.05 Hz scanning rate were used. Scans of 1 μm^2 fields (512 x 512 pixels) contained height-mode images of several dozens of top-view ("standing") 20S proteasome molecules. The gate status was deduced from a profile of raw height values of pixels measured by a probe scanning across the single proteasome particles. The proteasome α face that included the gate was completely rendered by a six-pixel (11-12 nm) scan-line fragment. When this scan-line presented a central dip (a local minimum), the particle was classified as containing the open gate. When a plot of height values presented a concave function without a local minimum, the particle was classified as an intermediate conformer. When the function was convex, the particle was classified as containing the closed gate.[13] The "events" of gate opening/closing were analysed for scans of distinct particles as well as multiple scans of the same particles.

Cell culture and Western Blotting. Human multiple myeloma RPMI 8226 cells and human monocyte-like U937 cells has been purchased from American Type Culture Collection (ATCC; Manassas, VA) and cultured according to ATCC specifications. The cells (passage 2-4) were treated with compound **3** or the vehicle diluted with the medium 1: 1000, for 48 hours. The content of live cells was determined by excluding the Trypan Blue-stained cells. The cells were counted with TC20 Automated Cell Counter (Bio-Rad Laboratories, Hercules, CA) and EC_{50} was calculated with Origin Pro 2017 (OriginLab Corporation, Northampton, MA). When indicated, the cells were harvested, washed twice in PBS, resuspended in dilution buffer and stored in -80°C. To prepare crude lysates the thawed preparations were vortexed with glass beads and centrifuged for 5 min 5,000xg (4°C). The supernatant was centrifuged for 20 min 14,000xg. The resulting supernatant was used as "crude lysate". SDS-PAGE was carried in 12% acrylamide, Tris-glycine gels from Invitrogen. Chameleon Duo (LI-COR Biosciences, Lincoln, NE) and Rainbow RPN800E (GE Healthcare, Chicago, IL) molecular weight standards were separated on each gel alongside lysates. The proteins were transferred to nitrocellulose membrane in a semi-dry system. The membranes were probed with specific primary antibodies from Cell Signaling Technology (Danvers, MA) (S6, PS6) and Li-Cor (COX IV), and then with secondary antibodies from Cell Signaling Technology. In each experiment visualization of S6, PS6 and COX IV was performed on the same membrane with Odyssey Infrared Imaging System (Cell Signalling Technology).

Conflicts of interest

The authors have no conflicts of interest with this work.

Acknowledgements

The work was supported by the William and Ella Owens Foundation for Medical Research (MG & PAO).

Notes and references

1 Bajorek, M., Finley, D. & Glickman, M. H. Proteasome disassembly and downregulation is correlated with viability during stationary phase. *Curr. Biol.*, 2003, **13**, 1140-1144.

2 Concannon, C. G., Koehler, B. F., Reimertz, C., Murphy, B. M., Bonner, C. *et al.* Apoptosis induced by proteasome inhibition in cancer cells: predominant role of the p53/PUMA pathway. *Oncogene*, 2007, **26**, 1681-1692.

3 Richardson, P. G. & Anderson, K. C. Bortezomib: a novel therapy approved for multiple myeloma. *Clin. Adv. Hematol. Oncol.*, 2003, **1**, 596-600.

4 Adams, J. The proteasome: a suitable antineoplastic target. *Nat. Rev. Cancer*, 2004, **4**, 349-360.

5 Kuhn, D. J., Orlowski, R. Z. & Bjorklund, C. C. Second generation proteasome inhibitors: carfilzomib and immunoproteasome-specific inhibitors (IPSIs). *Curr. Cancer Drug Targets*, 2011, **11**, 285-295.

6 Jankowska, E., Stoj, J., Karpowicz, P., Osmulski, P. A. & Gaczynska, M. The proteasome in health and disease. *Curr. Pharm. Des.*, 2013, **19**, 1010-1028.

7 Andreu-Vieyra, C. & Berenson, J. R. Carfilzomib in multiple myeloma. *Exp. Opin. Biol. Ther.*, 2014, **14**, 1685-1699.

8 Sprangers, R., Li, X., Mao, X., Rubinstein, J. L., Schimmer, A. D. *et al.* TROSY-based NMR evidence for a novel class of 20S proteasome inhibitors. *Biochemistry*, 2008, **47**, 6727-6734.

9 Gaczynska, M., Osmulski, P. A., Gao, Y., Post, M. J. & Simons, M. Proline- and arginine-rich peptides constitute a novel class of allosteric inhibitors of proteasome activity. *Biochemistry*, 2003, **42**, 8663-8670.

10 Andre, P., Groettrup, M., Klenerman, P., de Giuli, R., Booth, B. L., Jr. *et al.* An inhibitor of HIV-1 protease modulates proteasome activity, antigen presentation, and T cell responses. *Proc. Natl. Acad. Sci. USA*, 1998, **95**, 13120-13124.

11 Jones, C. L., Njomen, E., Sjogren, B., Dexheimer, T. S. & Tepe, J. J. Small Molecule Enhancement of 20S Proteasome Activity Targets Intrinsically Disordered Proteins. *ACS Chem. Biol.*, 2017, **12**, 2240-2247.

View Article Online
DOI: 10.1039/C9OB00122K

12 Osmulski, P. A. & Gaczynska, M. Rapamycin allosterically inhibits the proteasome. *Mol. Pharmacol.*, 2013, **84**, 104-113.
13 Gizynska, M., Witkowska, J. P., Karpowicz, P., Rostankowski, R., Chocron, E. S. *et al.* Proline- and arginine-rich peptides as flexible allosteric modulators of human proteasome activity. *J. Med. Chem.*, 2019, **62**, 359-370.
14 Gaczynska, M. & Osmulski, P. A. Harnessing proteasome dynamics and allostery in drug design. *Antioxid. Redox Signal.*, 2014, **21**, 2286-2301.
15 Li, X., Wood, T. E., Sprangers, R., Jansen, G., Franke, N. E. *et al.* Effect of noncompetitive proteasome inhibition on bortezomib resistance. *J. Natl. Cancer Inst.*, 2010, **102**, 1069-1082.
16 Vignot, S., Faivre, S., Aguirre, D. & Raymond, E. mTOR-targeted therapy of cancer with rapamycin derivatives. *Ann. Oncol.*, 2005, **16**, 525-537.
17 Liang, J., Choi, J. & Clardy, J. Refined structure of the FKBP12-rapamycin-FRB ternary complex at 2.2 A resolution. *Acta Christ. D*, 1999, **55**, 736-744.
18 Banaszynski, L. A., Liu, C. W. & Wandless, T. J. Characterization of the FKBP.rapamycin.FRB ternary complex. *J. Am. Chem. Soc.*, 2005, **127**, 4715-4721.
19 Ma, X. M. & Blenis, J. Molecular mechanisms of mTOR-mediated translational control. *Nat. Rev. Mol. Cell Biol.*, 2009, **10**, 307-318.
20 Groll, M., Bochtler, M., Brandstetter, H., Clausen, T. & Huber, R. Molecular machines for protein degradation. *Chembiochem*, 2005, **6**, 222-256.
21 Finley, D., Chen, X. & Walters, K. J. Gates, Channels, and Switches: Elements of the Proteasome Machine. *Trends Biochem. Sci.*, 2016, **41**, 77-93.
22 Ciechanover, A., Orian, A. & Schwartz, A. L. The ubiquitin-mediated proteolytic pathway: mode of action and clinical implications. *J. Cell Biochem. Suppl.*, 2000, **34**, 40-51.
23 Groll, M. & Potts, B. C. Proteasome structure, function, and lessons learned from beta-lactone inhibitors. *Curr. Top. Med. Chem.*, 2011, **11**, 2850-2878.
24 Schrader, J., Henneberg, F., Mata, R. A., Tittmann, K., Schneider, T. R. *et al.* The inhibition mechanism of human 20S proteasomes enables next-generation inhibitor design. *Science*, 2016, **353**, 594-598.
25 Osmulski, P. A., Hochstrasser, M. & Gaczynska, M. A tetrahedral transition state at the active sites of the 20S proteasome is coupled to opening of the alpha-ring channel. *Structure*, 2009, **17**, 1137-1147.
26 Forster, A., Masters, E. I., Whitby, F. G., Robinson, H. & Hill, C. P. The 1.9 A structure of a proteasome-11S activator complex and implications for proteasome-PAN/PA700 interactions. *Mol. Cell*, 2005, **18**, 589-599.
27 Ortega, J., Heymann, J. B., Kajava, A. V., Ustrell, V., Rechsteiner, M. *et al.* The axial channel of the 20S proteasome opens upon binding of the PA200 activator. *J. Mol. Biol.*, 2005, **346**, 1221-1227.
28 Gaczynska, M. & Osmulski, P., unpublished observations.
29 Hauske, J. R., Dorff, P., Julin, S., DiBrino, J., Spencer, R. *et al.* Design and synthesis of novel FKBP inhibitors. *J. Med. Chem.* , 1992, **35**, 4284-4296.
30 Feng, X., Sippel, C., Bracher, A. & Hausch, F. Structure-Affinity Relationship Analysis of Selective FKBP51 Ligands. *J. Med. Chem.*, 2015, **58**, 7796-7806.
31 Van Duyne, G. D., Standaert, R. F., Karplus, P. A., Schreiber, S. L. & Clardy, J. Atomic structure of FKBP-FK506, an immunophilin-immunosuppressant complex. *Science*, 1991, **252**, 839-842.
32 Meadows, R. P., Nettesheim, D. G., Xu, R. X., Olejniczak, E. T., Petros, A. M. *et al.* Three-dimensional structure of the FK506 binding protein/ascomycin complex in solution by heteronuclear three- and four-dimensional NMR. *Biochemistry*, 1993, **32**, 754-765.
33 Lepre, C. A., Thomson, J. A. & Moore, J. M. Solution structure of FK506 bound to FKBP-12. *FEBS Lett*, 1992, **302**, 89-96.
34 Dragovich, P. S., Barker, J. E., French, J., Imbacuan, M., Kalish, V. J. *et al.* Structure-based design of novel, urea-containing FKBP12 inhibitors. *J. Med. Chem.*, 1996, **39**, 1872-1884.
35 Smith, D. M., Chang, S. C., Park, S., Finley, D., Cheng, Y. *et al.* Docking of the proteasomal ATPases' carboxyl termini in the 20S proteasome's alpha ring opens the gate for substrate entry. *Mol. Cell*, 2007, **27**, 731-744.
36 Trott, O. & Olson, A. J. AutoDock Vina: improving the speed and accuracy of docking with a new scoring function, efficient optimization, and multithreading. *J. Comput. Chem.*, 2010, **31**, 455-461.
37 Dallakyan, S. & Olson, A. J. Small-molecule library screening by docking with PyRx. *Methods Mol. Biol.*, 2015, **1263**, 243-250.
38 Lander, G. C., Estrin, E., Matyskiela, M. E., Bashore, C., Nogales, E. *et al.* Complete subunit architecture of the proteasome regulatory particle. *Nature*, 2012, **482**, 186-191.
39 Dong, Y., Zhang, S., Wu, Z., Li, X., Wang, W. L. *et al.* Cryo-EM structures and dynamics of substrate-engaged human 26S proteasome. *Nature*, 2019, **565**, 49-55.
40 Gaczynska, M. & Osmulski, P. A. Atomic force microscopy of proteasome assemblies. *Methods Mol. Biol.*, 2011, **736**, 117-132.
41 Osmulski, P. A. & Gaczynska, M. Nanoenzymology of the 20S proteasome: proteasomal actions are controlled by the allosteric transition. *Biochemistry*, 2002, **41**, 7047-7053.
42 Chen, S., Wu, J., Lu, Y., Ma, Y. B., Lee, B. H. *et al.* Structural basis for dynamic regulation of the human 26S proteasome. *Proc. Natl. Acad. Sci. U S A*, 2016, **113**, 12991-12996.
43 Njomen, E., Osmulski, P. A., Jones, C. L., Gaczynska, M. & Tepe, J. J. Small Molecule Modulation of Proteasome Assembly. *Biochemistry*, 2018, **57**, 4214-4224.
44 Moss, W. O., Wakefield, E., Mahon, M. F., Mollowy, K. C., H., B. R. *et al.* Ketene-S,S-Acetals As 1,3-dipolarophiles Towards Azides. A New Synthetic Entry Into Cyclic Amino Acids. *Tetrahedron*, 1992, **48**, 7551-7564.
45 Martin, J., Deagostino, A., Perrio, C., Dauphin, F., Ducandas, C. *et al.* Syntheses of R and S isomers of AF-DX 384, a selective antagonist of muscarinic M2 receptors. *Bioorg. Med. Chem.*, 2000, **8**, 591-600.

View Article Online
DOI: 10.1039/C9OB00122K